A LOW-MACH LOW-REYNOLDS PRECONDITIONING SCHEME WITH PARTICULAR ATTENTION ON VISCOUS TIME-STEPPING

J. Fiedler and G. Ashcroft

Institute of Propulsion Technology
German Aerospace Center address
Linder Höhe
51147 Cologne
e-mail: {jens.fiedler, graham.ashcroft}@dlr.de

Keywords: convergence acceleration, compressible flows, viscous flows, low Mach preconditioning

Abstract. *Industrial design and optimization processes rely increasingly on powerful and well-engineered CFD tools. Compressible solution methods, which perform very well at transonic and supersonic flow speeds, display a dramatic degradation of convergence as well as of solution quality as the incompressibility limit is approached (very low flow speeds). In many technical applications, especially in turbomachinery, the flow conditions vary strongly within the computational domain and with time. When the incompressibility limit is approached, a large disparity arises between the smallest and largest eigenvalues of the systems characteristic matrix. In order to overcome these problems low-Mach preconditioning methods have been devised to rescale the eigenvalues of the characteristic matrix of the system of governing equations and, hence, reduce the large inequality in the acoustic and convective flow speeds. Frequently, low flow speeds are observed in low Reynolds environments. As noted by several authors, often instability issues in these regions, such as cavities and boundary layers, arise by preconditioning. Often, this problem is due to an overestimation of the maximum allowable timestep size. In fact, in a low Reynolds regime, the influence of viscous effects on time marching schemes predominates. An important role in the determination of viscous time steps plays the von Neumann number (VNN), whereas the Courant Friedrichs Lewy criteria (CFL) influences the inviscid time step behaviour.*

The objective of this work is the presentation of the theoretical background and results of a consistent Low-Mach preconditioning scheme based on a preconditioner proposed by Turkel, which has been extended to a wide range of Reynolds numbers. Furthermore, the interaction of low-Mach preconditioning, the von Neumann and Courant Friedrichs Lewy numbers on the convergence history and quality of results will be discussed. Its implementation is illustrated using DLR's in-house CFD code TRACE. To prove the robustness and correctness of the algorithm, we discuss a set of test cases like the lid-driven cavity at different Reynolds numbers influenced by CFL and VNN.

1 INTRODUCTION

Complex technical systems, such as turbomachinery configurations, involve large variations of different flow topologies. Some regions contain very low flow speeds whilst others are decidedly compressible. Exemplary, in the main flow passage of a turbomachinery configuration relatively high flow speeds dominate. Locally small Mach numbers can be found in cavity and seals regions. Numerical simulations of turbomachinery components are mostly performed by density-based flow solvers. At low flow speeds, fully compressible solution methods converge extremely slow, due to the large disparity between the convective and acoustic speeds. In addition, a dramatic degradation of the solution quality can by observed.

In order to overcome these problems, low-Mach preconditioning operators have been developed to reduce the difference between the largest and smallest eigenvalues of the system's characteristic matrix [1]. Pre-multiplication of the time derivative of the Euler or Navier-Stokes system of equations by a suitable matrix rescales the various characteristic velocities. Preconditioning does not only reduce the stiffness of the system but also significantly increase the accuracy at low flow speeds. In the past, several preconditioning operators have been published, e.g. [10, 1, 12, 13]. A comprehensive overview of the low Mach preconditioning operators, developed during the last decades, can be found in the work of Depcik [2]. As noted by several authors low-Mach preconditioning can cause stability problems in viscous regimes [3, 6]. This is due to overestimation of the maximum allowable timestep size. In fact, in a low Reynolds regime the time steps are predominated by the viscous eigenvalues. This aspect of preconditioned flows has been discussed previously by Choi and Merkle [13] as well as Colin *et. al* [6]. Based on stability investigations the significant influence of viscosity on low Mach preconditioning has been proven. Based on a preconditioner proposed by Turkel [1], in this paper we discuss the influence of an additional limitation term of the preconditioning parameter β^2 on the numerical stability in a viscous environment, cf. [3, 6].

Moreover, the validity and robustness of the method is demonstrated using a classical lid-driven cavity configuration at different Reynolds, CFL and von Neumann numbers.

The improvements has been implemented in the CFD code TRACE, a fully implicit, parallel, hybrid, multi-block, Reynolds-Averaged Navier-Stokes flow solver specialised in the simulation of turbomachinery flows [5].

2 NUMERICAL METHOD

The non-dimensional time-dependent Navier-Stokes equations formulated in Cartesian coordinates read [4]

$$\frac{\partial \mathbf{Q}}{\partial t} + \frac{\partial \mathbf{f}}{\partial x} + \frac{\partial \mathbf{g}}{\partial y} + \frac{\partial \mathbf{h}}{\partial z} = \frac{1}{Re_a} \left(\frac{\partial \mathbf{f}_\nu}{\partial x} + \frac{\partial \mathbf{g}_\nu}{\partial y} + \frac{\partial \mathbf{h}_\nu}{\partial z} \right), \tag{1}$$

where $\mathbf{Q}$ is the solution vector of the conservative variables $(\rho, \rho u, \rho v, \rho w, \rho E)$ and $\mathbf{f}$, $\mathbf{g}$, $\mathbf{h}$ the inviscid fluxes given by, cf. [6]:

$$\mathbf{f} = \begin{pmatrix} \rho u \\ \rho u^2 + p \\ \rho uv \\ \rho uw \\ \rho uH \end{pmatrix}, \quad \mathbf{g} = \begin{pmatrix} \rho v \\ \rho vu \\ \rho v^2 + p \\ \rho vw \\ \rho vH \end{pmatrix}, \quad \mathbf{h} = \begin{pmatrix} \rho w \\ \rho wu \\ \rho wv \\ \rho w^2 + p \\ \rho wH \end{pmatrix}, \tag{2}$$

2

where ρ, u, v, w and p are the density, velocities and pressure, respectively. The quantities H and E are the specific total enthalpy and energy. The viscous fluxes are given by

$$
\mathbf{f}_\nu = \begin{pmatrix} 0 \\ \tau_{xx} \\ \tau_{xy} \\ \tau_{xz} \\ (\tau U)_x) \end{pmatrix}, \quad
\mathbf{g}_\nu = \begin{pmatrix} 0 \\ \tau_{yx} \\ \tau_{yy} \\ \tau_{yz} \\ (\tau U)_y) \end{pmatrix}, \quad
\mathbf{h}_\nu = \begin{pmatrix} 0 \\ \tau_{zx} \\ \tau_{zy} \\ \tau_{zz} \\ (\tau U)_z) \end{pmatrix}.
\tag{3}
$$

The components of the viscous stress tensor are referred to as τ_{ij} where $i, j = x, y, z$. The vector U contains the Cartesian velocity components. Source terms and heat flux contributions are not in the focus of the current work and have therefore been ignored. The fluid is considered as calorically perfect. Hence, the ratio of the specific heats is constant and set to 1.4. The acoustic Reynolds number is defined by

$$
Re_a = \frac{\rho^* a^* L^*}{\mu^*},
\tag{4}
$$

where ρ^*, a^*, L^*, μ^* are the (dimensional) reference density, speed of sound, length and viscosity. The system of equations (1) is spatially discretized using Roe's upwind approximation scheme [17]. The (preconditioned) inviscid fluxes at the cell faces are computed as

$$
\mathbf{F}_{i+1/2} = \frac{1}{2} \left(\mathbf{F}_L + \mathbf{F}_R \right) - \frac{\partial \mathbf{Q}}{\partial \mathbf{U}} \mathbf{P}_U^{-1} |\mathbf{P}_U \mathbf{D}_U| \frac{\partial \mathbf{U}}{\partial \mathbf{Q}} \left(\mathbf{Q}_L - \mathbf{Q}_R \right),
\tag{5}
$$

where $\mathbf{Q}_L$ and $\mathbf{Q}_R$ are the states at the left and right side of the cell face. The term $\mathbf{P}_U^{-1} |\mathbf{P}_U \mathbf{D}_U|$, where $\mathbf{D}_U = \kappa \cdot \frac{\partial \mathbf{F}}{\partial \mathbf{U}}$, is known as the stabilisation term and leads after a matrix decomposition of the flux Jacobians, to $\mathbf{P}_U^{-1} \mathbf{M}_U |\mathbf{\Lambda}| \mathbf{M}_U^{-1}$. The primitive variable system (ρ, u, v, w, p) is denoted as U. Based on a metric proposed by Hirsch [4] the preconditioned left and right eigenvector matrices are

$$
\mathbf{M}_U^{-1} = \begin{pmatrix}
\hat{\kappa}_x & 0 & \hat{\kappa}_z & -\hat{\kappa}_y & -\hat{\kappa}_x \frac{1}{a^2} \\
\hat{\kappa}_y & -\hat{\kappa}_z & 0 & \hat{\kappa}_x & -\hat{\kappa}_y \frac{1}{a^2} \\
\hat{\kappa}_z & \hat{\kappa}_y & -\hat{\kappa}_x & 0 & -\hat{\kappa}_z \frac{1}{a^2} \\
0 & \hat{\kappa}_x & \hat{\kappa}_y & \hat{\kappa}_z & -\frac{\hat{\lambda}_1 - \hat{\lambda}_4}{\beta^2 a^2 \rho} \\
0 & -\hat{\kappa}_x & -\hat{\kappa}_y & -\hat{\kappa}_z & \frac{\hat{\lambda}_1 - \hat{\lambda}_5}{\beta^2 a^2 \rho}
\end{pmatrix}
\tag{6}
$$

$$
\mathbf{M}_U = \begin{pmatrix}
\hat{\kappa}_x & \hat{\kappa}_y & \hat{\kappa}_z & \frac{\rho \beta^2}{\hat{\lambda}_4 - \hat{\lambda}_5} & \frac{\rho \beta^2}{\hat{\lambda}_4 - \hat{\lambda}_5} \\
0 & -\hat{\kappa}_z & \hat{\kappa}_y & \hat{\kappa}_x \frac{\hat{\lambda}_1 - \hat{\lambda}_5}{\hat{\lambda}_4 - \hat{\lambda}_5} & \hat{\kappa}_x \frac{\hat{\lambda}_1 - \hat{\lambda}_4}{\hat{\lambda}_4 - \hat{\lambda}_5} \\
\hat{\kappa}_z & 0 & -\hat{\kappa}_x & \hat{\kappa}_y \frac{\hat{\lambda}_1 - \hat{\lambda}_5}{\hat{\lambda}_4 - \hat{\lambda}_5} & \hat{\kappa}_y \frac{\hat{\lambda}_1 - \hat{\lambda}_4}{\hat{\lambda}_4 - \hat{\lambda}_5} \\
-\hat{\kappa}_y & \hat{\kappa}_x & 0 & \hat{\kappa}_z \frac{\hat{\lambda}_1 - \hat{\lambda}_5}{\hat{\lambda}_4 - \hat{\lambda}_5} & \hat{\kappa}_z \frac{\hat{\lambda}_1 - \hat{\lambda}_4}{\hat{\lambda}_4 - \hat{\lambda}_5} \\
0 & 0 & 0 & \frac{\rho \beta^2 a^2}{\hat{\lambda}_4 - \hat{\lambda}_5} & \frac{\rho \beta^2 a^2}{\hat{\lambda}_4 - \hat{\lambda}_5},
\end{pmatrix}
\tag{7}
$$

where κ_x, κ_y and κ_z are the metric components. The preconditioning operator $\mathbf{P}_U$ and its

3

inverse $\mathbf{P}_U^{-1}$, proposed by Turkel [10] and formulated in primitive variables, reads

$$
\mathbf{P}_U^{-1} = \begin{pmatrix} 1 & 0 & 0 & 0 & -\frac{\beta^2-1}{a^2\beta^2} \\ 0 & 1 & 0 & 0 & 0 \\ 0 & 0 & 1 & 0 & 0 \\ 0 & 0 & 0 & 1 & 0 \\ 0 & 0 & 0 & 0 & \beta^{-2} \end{pmatrix} \qquad \mathbf{P}_U = \begin{pmatrix} 1 & 0 & 0 & 0 & \frac{\beta^2-1}{a^2} \\ 0 & 1 & 0 & 0 & 0 \\ 0 & 0 & 1 & 0 & 0 \\ 0 & 0 & 0 & 1 & 0 \\ 0 & 0 & 0 & 0 & \beta^2 \end{pmatrix} \tag{8}
$$

The diagonal matrix $\mathbf{\Lambda}$ contains the (preconditioned) normalised eigenvalues which are given by

$$
\hat{\lambda}_{1,2,3} = u\hat{\kappa}_x + v\hat{\kappa}_y + w\hat{\kappa}_z \tag{9}
$$

$$
\hat{\lambda}_{4,5} = \frac{1}{2}\left(1+\beta^2\right)\hat{\lambda}_1 \pm \frac{1}{2}\sqrt{(1-\beta^2)^2\,\hat{\lambda}_1^2 + 4\beta^2 a^2} \tag{10}
$$

The components of the metric vector have been normalised by

$$
\hat{\kappa}_i = \frac{\kappa_i}{\|\kappa\|} \tag{11}
$$

which results in

$$
\hat{\lambda}_i = \frac{\lambda_i}{\|\kappa\|} \tag{12}
$$

The system of equations (1) is temporally discretised by a first order Euler backward discretisation scheme. Within this work steady state cases have been considered only and a pseudo-time step τ has been introduced to control the residual behaviour, cf. [8] The preconditioning operator modifies the pseudo-time τ and the residual $\mathbf{R}$. Therefore, the update vector $\triangle\mathbf{Q}$ at time step m reads

$$
\triangle\mathbf{Q} = -\mathbf{R}^m \left(\frac{\mathbf{P}_Q^{-1}}{\triangle\tau} + \left.\frac{\partial\mathbf{R}}{\partial\mathbf{Q}}\right|^m \right)^{-1} \tag{13}
$$

The pseudo-time step $\triangle\tau_i$ considered for a cell i is determined by applying the CFL condition

$$
\triangle\tau_i = CFL\frac{\triangle h_i}{\lambda_{4,i} + \delta\frac{CFL}{VNN}\lambda_{\nu,i}} \tag{14}
$$

where $\triangle h_i$ is a characteristic length of the cell volume, $\lambda_{4,i}$ is given by (10) and $\lambda_{v,i}$ is defined by [7, 14]

$$
\lambda_{\nu,i} = \max\left(\frac{4}{3\rho}, \frac{\gamma}{\rho}\right)\left(\frac{\mu_L}{Pr_L} + \frac{\mu_T}{Pr_T}\right)\frac{1}{\triangle h_i}, \tag{15}
$$

where Pr_L and Pr_T are the laminar and turbulent Prandtl numbers. The laminar and turbulent dynamic viscosity coefficients are denoted by μ_L and μ_T, respectively. For purely inviscid consideration $\delta = 0$.

4

The preconditioning parameter β^2 is related to the local Mach number M and is initially defined as [6]

$$\beta^2 = \min\left(\max\left(M^2, \beta_{min}^2\right), 1\right).\tag{16}$$

In order to avoid singularities in the preconditioning matrices β_{min}^2 should be set to some appropriate value. Moreover, the choice of β_{min}^2 strongly influences the stability of the pre-conditioned system. As stated by several authors [1, 15], β_{min}^2 should not be extremely small compared to the general flow velocity. Turkel [1] suggests to set β_{min}^2 to $K_1 M_{ref}^2$, where K_1 is a problem-dependent constant and M_{ref} a reference Mach number, i.e. often the inflow Mach number. In the current investigations $\beta_{min}^2 = 10^{-5}$. In the vicinity of stagnation points the local Mach number approaches zero. Darmofal and Siu [11] suggests to limit β^2 additionally by the local pressure gradient $K_2 \max\limits_{faces}\left(|\triangle p|/\rho a^2\right)$, where $\triangle p = p_r - p_l$ and p_r and p_l are the pressures of the particular states and K_2 is a problem-dependent constant. Hence, β^2 reads

$$\beta^2 = \min\left(\max\left(M^2, \beta_{min}^2, K_2\max_{faces}\left(\frac{|\triangle p|}{\rho a^2}\right)\right), 1\right).\tag{17}$$

Venkateswaran [3] suggests to limit β^2 at low Re numbers using the diffusion velocity defined by

$$v_{vis} = \frac{\nu}{\triangle x},\tag{18}$$

where ν is the kinematic viscosity related to the dynamic viscosity μ via $\nu = \mu/\rho$. Hence,

$$v_{vis} = \frac{\mu}{\rho\triangle x}\tag{19}$$

In order to determine a low Reynolds limit for β^2 the viscous Mach number is introduced by

$$M_{vis} = \frac{v_{vis}}{a}.\tag{20}$$

Within the current work, the results above have been combined to obtain

$$\beta^2 = \min\left(\max\left(M^2, \beta_{min}^2, K_2\max_{faces}\left(\frac{|\triangle p|}{\rho a^2}\right), M_{vis}^2\right), 1\right).\tag{21}$$

The discretised algebraic system of equations has been solved using a symmetric Gauss-Seidel algorithm (SGS) and a predictor-corrector Gauss-Seidel scheme (PC-SGS). All calculations have been performed in double precision.

3 RESULTS

The lid-driven cavity configuration has been chosen to prove the correctness and accuracy of the algorithm. Often, this problem serves as a benchmark for the incompressible Navier-Stokes equations [18, 16]. Despite its simple setup, it allows a wide range of numerical properties and stability issues to be studied. Depending on the Reynolds number, the flows are characterised by multiple counter rotating recirculation regions in the corners of the cavity. The computational domain consists of a square where the upper wall moves at a constant horizontal velocity. All

walls are considered adiabatic. The Reynolds number considered within this configuration is defined by

$$Re_1 = \frac{\rho^* u^*_{Wall} L^*}{\mu^*}. \tag{22}$$

Numerical studies have been performed modifying the Reynolds number Re_1 by varying the reference length L^*. The latter scales the size of the configuration keeping u^*_{Wall} constant and therefore the velocity distribution within the domain over the whole range of Re_1.

For Re_1 = 1000 grid independency studies have been carried out for different mesh sizes generated by successive refinement. Figures (5) and (6) show the v-velocity profiles along a horizontal line and the u-velocity profiles along a vertical line passing through the centre of the cavity. The results are in very good agreement with those obtained by Ghia *et. al.* [18]. Based on the mesh resolution results the computational grid is set to 81 x 81 cells without refinement at the walls.

The streamlines computed at Reynolds number Re_1 = 1 and Re_1 = 100 are shown in figures (1) and (3). Low-mach preconditioning does not show to have a significant influence on the results but provide a higher convergence rate at low CFL numbers, see figures (2) and (4). Calculations have been performed with CFL = 1 and CFL = 25. Both, the preconditioned and non-preconditioned solutions are in very good agreement with those published in the available literature, e.g [13].

In contrast to the non-preconditioned calculations obtained at $Re_1 = 1$ and $Re_1 = 100$ the quality of the results for $Re_1 = 1000$ presented in figure (7a) are not in accordance to those computed by low Mach preconditioning, see figure (7c). The solution quality has been considerably improved using a low Mach preconditioning technique. The influence of M_{vis} on the numerical stability of a preconditioned calculation have been studied with SGS and PC-SGS. The solution quality diminishes drastically using a low Mach preconditioned SGS without additional modifications for low Reynolds environments as predicted by equation (21), figures (8) and (7b). The secondary recirculation patterns at the corners of the cavity are inadequately formed. The improvement in numerical stability through M_{vis} on a low-Mach preconditioned predictor-corrector scheme is less important, but clearly recognisable, see figure (9). This emphasis the necessity to limit β^2 by M_{vis} at low Reynolds numbers.

Low Mach preconditioning alleviates the strong disparity between the smallest and largest eigenvalues. Consequently, in low Reynolds regions it is inappropriate to use a purely inviscid scheme as the smaller the largest convective eigenvalue becomes the more important the largest viscous eigenvalue in a viscous regime becomes. Therefore, the convergence rate is no longer primarily determined by the low Mach preconditioner and CFL number but rather by the von Neumann number and largest viscous eigenvalue. Figures (10) and (11) present the convergence history of a lid-driven cavity calculation at $Re_1 = 1000$ at constant CFL and increasing VNN number up-to 10. Clearly, the viscous eigenvalue strongly alters the convergence rate but, based on the current configuration, has only a minor impact on the solution quality.

4 CONCLUSIONS

The numerical stability of a low-Mach preconditioned scheme is strongly influenced by a low-Reynolds modification of the preconditioning parameter β. In this work a consistent formulation of a preconditioning scheme applicable to a wide range of Reynolds and Mach numbers has been presented in the context of a fully-implicit three-dimensional compressible Navier-Stokes flow solver demonstrated. The validity has been proved using a classical lid-driven

cavity configuration. The influence of viscous timestep size has been studied and its impact on convergence rate shown. Moreover, for the configuration chosen in this work the viscous eigenvalues alter the computational result only slightly. In future work it is planned to investigate the viscous timestep behaviour depending on the ratio (CFL/VNN) and low-Mach preconditioning on different computational configurations.

REFERENCES

[1] E. Turkel, Preconditioning techniques in computational fluid dynamics. *Annu. Rev. Fluid. Mech.*, **31**, 385–416, 1999

[2] Ch. D. Depcik, A perfect local preconditioner for the Navier-Stokes equations. *Master Thesis*, University of Michigan, 2002

[3] S. Venkateswaran and L. Merkle, Analysis of preconditioning methods for the Euler and Navier-Stokes equations. *von Kármán Institute for Fluid Dynamics, Lecture Series*, 1999

[4] Ch. Hirsch, *Numerical Computation of Internal and External Flows*. John Wiley & Sons, Ltd., 2007

[5] K. Becker, K. Heitkamp and E. Kügeler, Recent progress in a hybrid-grid CFD solver for turbomachinery flows. *Proceedings of the 5th European Congress on Computational Methods in Applied Science and Engineering (ECCOMAS 2010), Lisbon, Portugal, June 2010*

[6] Y. Colin, H. Deniau and J.-F. Boussuge, A robust low speed preconditioning formulation for viscous flow computations. *Computer & Fluids*, **47**, 1–15, 2011.

[7] R. C. Swanson, E. Turkel and J. A. White, An effective multigrid method for high-speed flows. *NASA CR-187602*, 1991.

[8] A. Jamenson, Time-dependent calculations using multigrid, with applications to unsteady flow past airfoils and wings. *AIAA-91-GT-1596*, 1991

[9] P. L. Roe, Approximative Riemann solvers, parameter vectors and difference schemes. *J. Comput. Phys.*, **43**, 1981

[10] E. Turkel, Preconditioned Methods for Solving the Incompressible and Low-Speed Compressible Equations. *J. Comput. Phys.*, **72**, 1987

[11] D. L. Darmofal and K. Siu, A robust multigrid algorithm for the Euler equations with local preconditioning and semi-coarsing. *J. Comput. Phys.*, **151**, 1999

[12] J. M. Weiss and W. A. Smith, Preconditioning applied to variable and constant density flows. *AIAA Journal*, **33**

[13] Y.-H. Choi and C. L. Merkle, The application of preconditioning in viscous flows. *J. Comput. Phys.*, **105**, 1993

[14] S. Abarbanel and D. Gottlieb, Optimal time splitting for two- and three-dimensional Navier-Stokes equations with mixed derivatives. *J. Comput. Phys.*, **41**, 1981

[15] D. L. Darmofal and P. J. Schmid, The importance of eigenvectors for local preconditioners of the Euler equations. *J. Comput. Phys.*, **127**, 1996

[16] E. Erturk, Discussions on driven cavity flow. *Int. J. Numer. Meth. Fl.*, **60**, 275–294, 2008

[17] P. L. Roe, Approximative Riemann solvers, parameter vectors and difference schemes. *J. Comput. Phys.*, **43**, 357–372, 1981

[18] U. Ghia, K. N. Ghia and C. T. Shin, High-Re solutions for incompressible flow using the Navier-Stokes equations and a multigrid methods. *J. Comput. Phys.*, **48**, 387–411, 1982
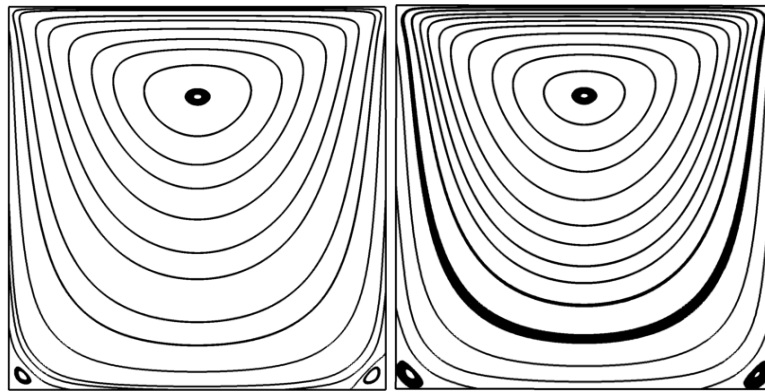
Figure 1: Streamlines in non-preconditioned (left) and preconditioned (right) calculations of a lid-driven cavity configuration for $Re_1 = 1$, CFL = 25 and VNN = 0.
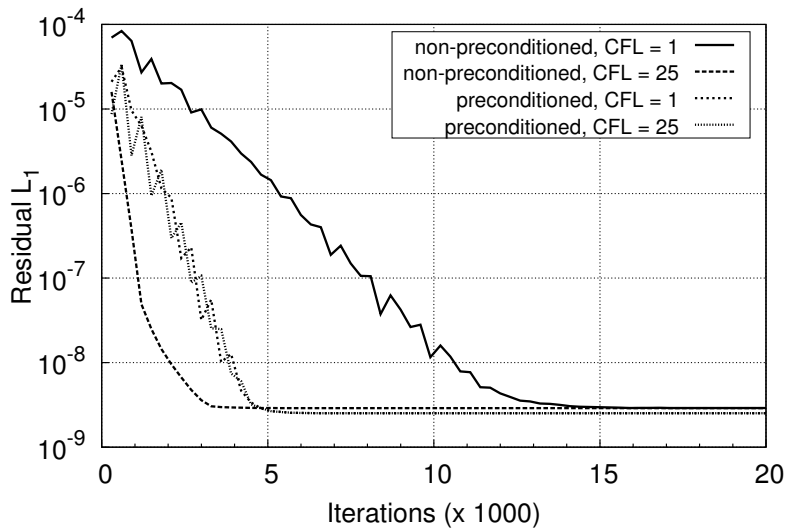
Figure 2: L_1 Residual for $Re_1 = 1$ obtained with CFL = 1, 25 and VNN = 0.

8
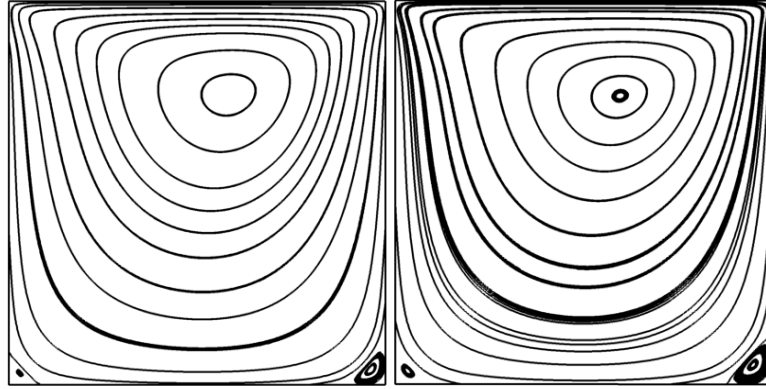
Figure 3: Streamlines in non-preconditioned (left) and preconditioned (right) calculations of a lid-driven cavity configuration for $Re_1 = 100$, CFL = 25 and VNN = 0.
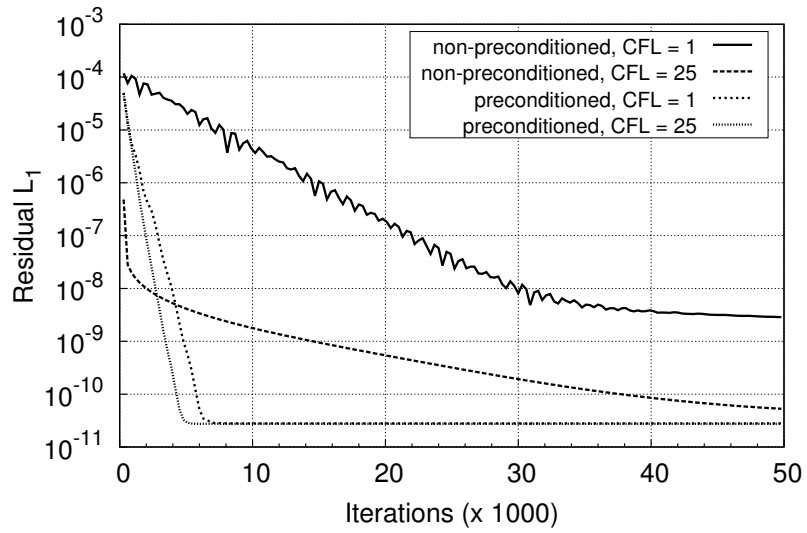
Figure 4: L_1 Residual for $Re_1 = 100$ obtained with CFL = 1, 25 and VNN = 0.
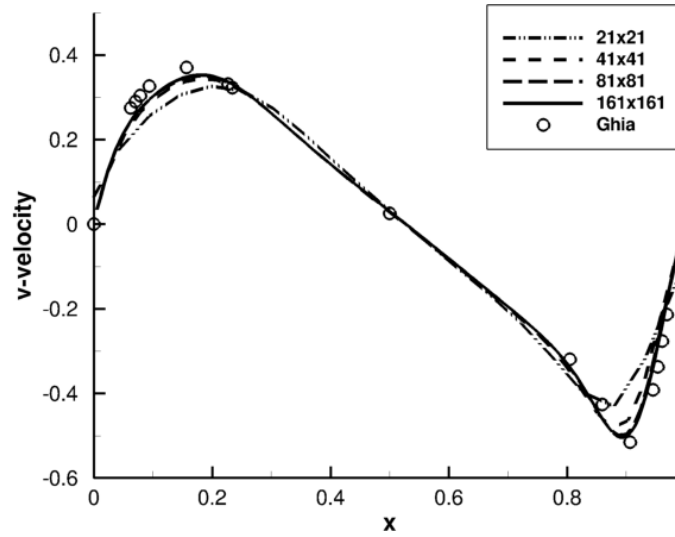
Figure 5: V-velocity profiles of a low-Mach preconditioned calculation along a horizontal line passing through the centre of the cavity at $Re_1 = 1000$, CFL = 25 and VNN = 0.
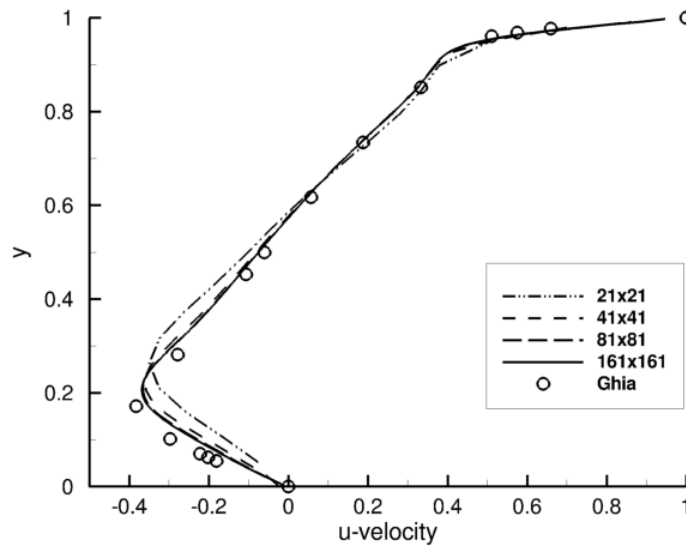
Figure 6: U-velocity profiles of a low-Mach preconditioned calculation along a vertical line passing through the centre of the cavity at $Re_1 = 1000$, CFL = 25 and VNN = 0.
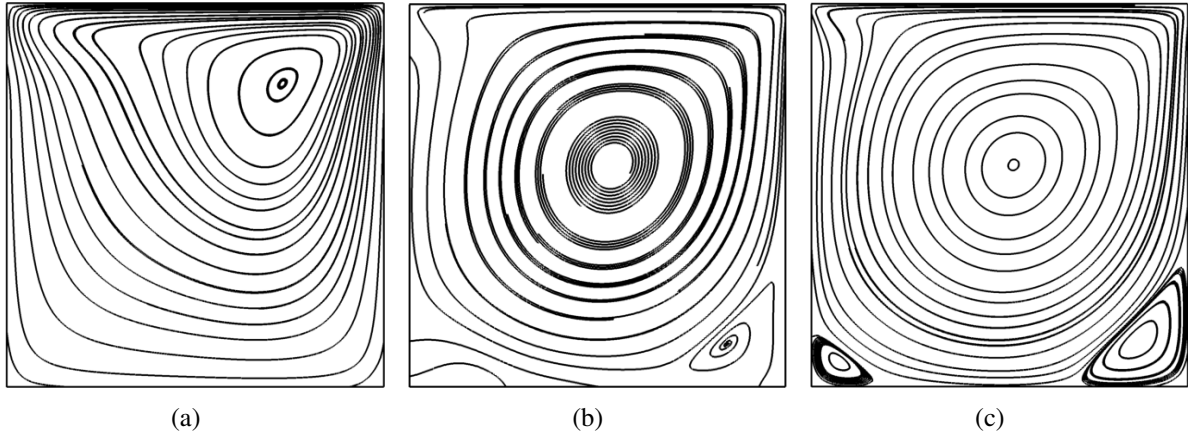
Figure 7: Streamlines in a non-preconditioned (7a), a preconditioned calculation without (7b) and with low Reynolds modification (7c) of β^2 using a symmetric Gauss-Seidel solution scheme (SGS) for $Re_1 = 1000$, CFL = 25 and VNN = 0.
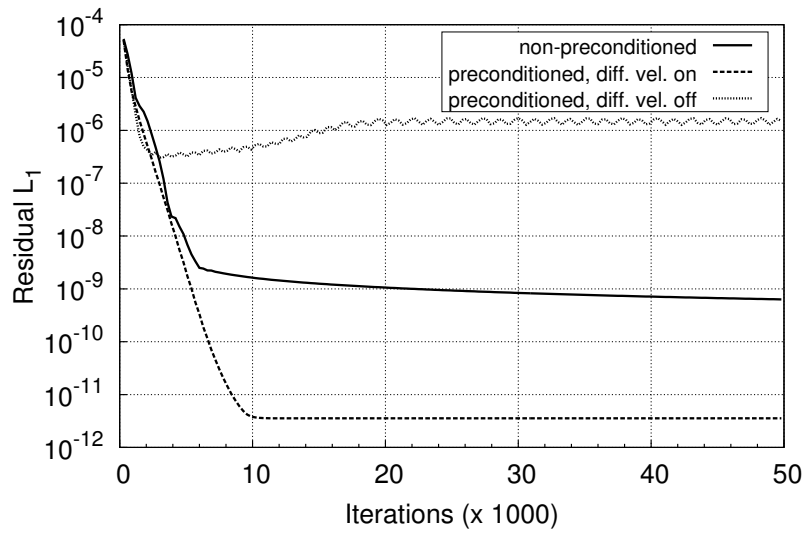
Figure 8: Influence of M_{vis} on the numerical stability of a symmetric Gauss-Seidel solution scheme (SGS) for $Re_1 = 1000$, CFL = 25 and VNN = 0.
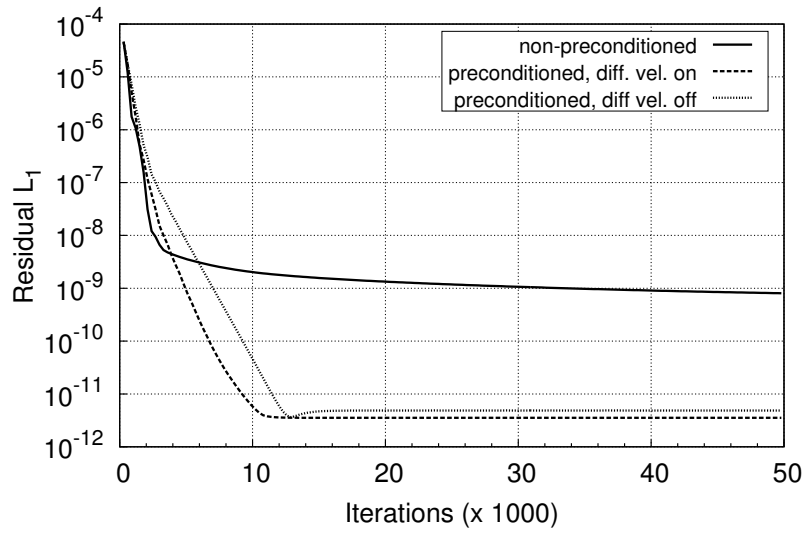
Figure 9: Influence of M_{vis} on the numerical stability of a low Mach preconditioned predictor-corrector Gauss-Seidel method (PC-SGS) for $Re_1 = 1000$, CFL = 25 and VNN = 0.
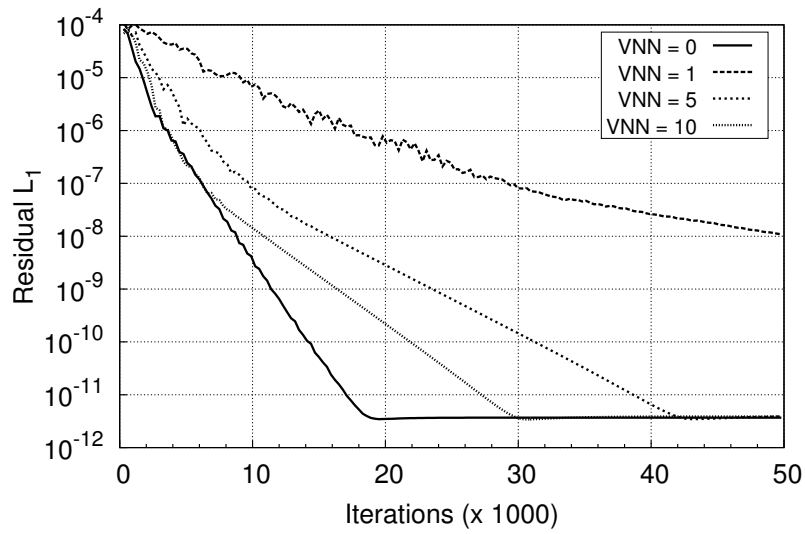
Figure 10: L_1 residual at increasing VNN of a low Mach preconditioned predictor-corrector Gauss-Seidel method (PC-SGS) at CFL = 1 and $Re_1 = 1000$.

12
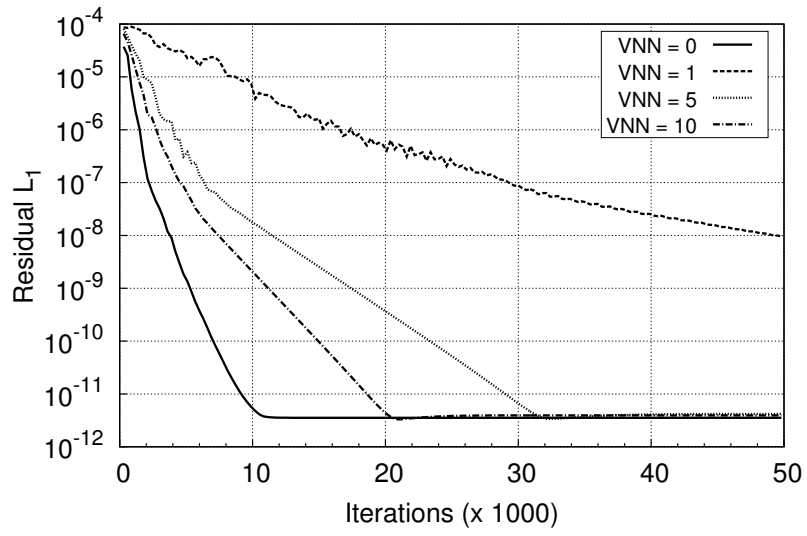
Figure 11: L_1 residual at increasing VNN of a low Mach preconditioned predictor-corrector Gauss-Seidel method (PC-SGS) at CFL = 10 and $Re_1 = 1000$.